ELSEVIER

Journal of Nuclear Materials 283–287 (2000) 1448–1452

journal of nuclear materials

www.elsevier.nl/locate/jnucmat

Experimental study on beryllium-7 production via sequential reactions in lithium-containing compounds irradiated by 14 MeV neutrons

F. Maekawa [a,*], Y.M. Verzilov [b], D.L. Smith [c], Y. Ikeda [a]

[a] *Japan Atomic Energy Research Institute, Fusion Neutronics Laboratory, Tokai-mura, Naka-gun, Ibaraki-ken, 319-1195 Japan*
[b] *Moscow State Engineering Physics Institute, Kashirskoe Shosse 31, Moscow 115409, Russian Federation*
[c] *Argonne National Laboratory, Argonne, IL 60439, USA*

Abstract

Except for ^{3}H and ^{14}C, no radioactive nuclide is produced by neutron-induced reactions with lithium in lithium-containing materials such as Li_2O and Li_2CO_3. However, when the lithium-containing materials are irradiated by 14 MeV neutrons, radioactive ^{7}Be is produced by sequential charged particle reactions (SCPR). In this study, we measured effective ^{7}Be production cross-sections in several lithium-containing samples at 14 MeV: the cross-sections are in the order of μb. Estimation of the effective cross-sections is attempted, and the estimated values agreed well with the experimental data. It was shown that the ^{7}Be activity in a unit volume of lithium-containing materials in D-T fusion reactors can exceed total activity of the same unit volume of the SiC structural material in a certain cooling time. Consequently, a careful consideration of the ^{7}Be production by SCPR is required to assess radioactive inventories in lithium-containing D-T fusion blanket materials.

1. Introduction

No radioactive nuclide except for tritium is produced from stable lithium isotopes, i.e., lithium-6 and lithium-7, by 14 MeV neutron-induced nuclear reactions. When we irradiate lithium-containing materials by 14 MeV neutrons, however, we will observe 478 keV γ-rays from beryllium-7 which has a half-life of 53 days. The beryllium-7 is produced via sequential charged particle reactions (SCPR); energetic protons, deuterons and tritons (charged particle, CP) are first produced by 14 MeV neutron interactions with nuclei in the materials, and the CPs then induce the beryllium-7 production reactions such as $^{7}Li(p,n)^{7}Be$ and $^{6}Li(d,n)^{7}Be$. Radioactive nuclides produced by SCPR may be an additional source of the inventory of radioactive nuclides in materials irradiated in a fusion neutron environment. Most of the inventory calculation codes deal with only neutron-induced reactions but not SCPR. In some cases, radioactive nuclides produced by the SCPR contribute significantly to the total inventory of radioactive nuclides. The beryllium-7 production by SCPR in lithium-containing materials is one such example.

The FISPACT code [1] can treat SCPR with an algorithm [2] developed by Cierjacks et al. The beryllium-7 production, however, seems very difficult to predict with FISPACT. By neutron interactions, CPs are produced by the break-up reactions of lithium nuclei which require very detailed knowledge of each break-up reaction path while the FISPACT code adopts a completely different model to calculate energy spectra of CPs, i.e., the statistical evaporation model. Therefore, experimental study of SCPR is required especially for lithium-containing materials. The experimental SCPR cross-sections are very limited: those for vanadium, iron and copper reported by Ikeda et al. [3] are the only available experimental data for 14 MeV neutrons.

* Corresponding author. Tel.: +81-29 282 6948; fax: +81-29 282 6496.
E-mail address: fujio@fnshp.tokai.jaeri.go.jp (F. Maekawa).

0022-3115/00/$ - see front matter
PII: S0022-3115(00)00182-3

In this work, we measured the effective beryllium-7 production cross-sections at 14 MeV in some lithium-containing samples. Calculational estimation of the cross-sections was attempted, and the estimated values were compared with the experimental data. Finally, the impact of the produced beryllium-7 activity on a fusion reactor was investigated.

2. Experiment

Chemical compounds treated in this study are summarized in Table 1. They were lithium oxide, lithium carbonate and lithium hydroxide with three different lithium enrichments: lithium-6 enriched, lithium-7 enriched and natural abundance. Pellet samples of 12 mm in diameter and about 2 mm in thickness were produced from powder samples for all the chemical compounds. Masses of all the pellets ranged between 0.35 and 0.46 g.

As shown in Fig. 1, three pellets were stacked. The center was the main pellet for which ^{7}Be activity was to be measured after D–T neutron irradiation. The two pellets were attached to both sides of the central pellet to simulate the central pellet residing in an infinite medium in terms of ranges of CPs. Note that ranges of CPs produced in the pellets were at most 1.0 mm; that is less than the pellet thickness of about 2 mm. The pellet stack was wrapped in an aluminum foil. Niobium foils of $5 \times 5 \times 0.5$ mm^3, which were used as neutron fluence monitors, were attached on both sides of the stack.

Table 1
Samples and measured effective ^{7}Be production cross-section

Sample	Enrichment (%)	Effective ^{7}Be production cross-section (μb)
$^{6}Li_2CO_3$	^{6}Li: 95.4	16 ± 1
$^{7}Li_2CO_3$	^{7}Li: 99.95	13 ± 1
$^{nat}Li_2CO_3$	^{7}Li: 92.5	15 ± 1
^{6}LiOH	^{6}Li: 95.4	35 ± 3
^{7}LiOH·H_2O	^{7}Li: 99.95	681 ± 40
^{nat}LiOH·H_2O	^{7}Li: 92.5	593 ± 36
$^{6}Li_2O$	^{6}Li: 95.4	49 ± 3
$^{7}Li_2O\cdot(H_2O)_{0.090}$	^{7}Li: 99.95	67 ± 4
$^{nat}Li_2O\cdot(H_2O)_{0.106}$	^{7}Li: 92.5	55 ± 4

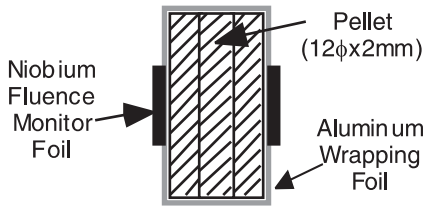

Fig. 1. Pellet sample stack for irradiation.

The fusion neutronics source (FNS) facility [4] in the Japan Atomic Energy Research Institute was used for neutron irradiation. The sample stacks were placed at 45 mm from the neutron source, and irradiated by 14.6 MeV neutrons for 150 h. Typical neutron fluence in the irradiation was 4×10^{15} n/cm^2. After 1–2 month(s), the 478 keV γ-rays from beryllium-7 produced in the central pellets were measured by a high-purity germanium (HP-Ge) detector. The 935 keV γ-rays emitted from the niobium monitor foils were also measured, and total 14 MeV neutron fluence for each pellet was determined by using the ^{93}Nb(n,2n)^{92m}Nb reaction rates. The effective beryllium-7 production cross-sections were deduced from the measured peak counts and necessary data such as the decay constant of ^{7}Be (0.01301 1/day), the γ-ray intensity per decay (10.39%), detection efficiency of HP-Ge detector for the 478 keV γ-ray (2.29%), sample masses, etc.

Major experimental error sources were statistical errors of the peak counts for the 478 keV γ-ray (1–3%), the detection efficiency of HP-Ge detector (3%) and uncertainty associated with the neutron fluence for the central pellets (5%). Overall experimental errors ranged between 5% and 7%. Table 1 summarizes the measured results.

3. Estimation of the effective cross-section

3.1. Formulation of SCPR

The effective ^{7}Be production cross-section was estimated as follows: when we consider a CP production reaction for a target nuclide A at a certain energy (14 MeV for example), A(n,CP), the energy distribution of the CPs produced in a unit volume $S_{CP}(E_{CP})$ (CPs/cm^3/MeV) is calculated as

$$S_{CP}(E_{CP}) = \phi_n N_A \sigma_{CP} P(E_{CP}), \tag{1}$$

where ϕ_n (1/cm^2) is the neutron flux, N_A (1/cm^3) is the atomic density of A, σ_{CP} (cm^2) is the CP production cross-section of A and $P(E_{CP})$ (1/MeV) is a normalized CP spectrum. The CPs form a CP flux $\phi_{CP}(E)$ (1/cm^2/MeV) in the material when CPs slowed down:

$$\phi_{CP}(E) = \{dE/dx(E)\}^{-1} \int_E^{E_{max}} S_{CP}(E_{CP})\, dE_{CP}, \tag{2}$$

where $dE/dx(E)$ (MeV/cm) is stopping power of the material.

We think of a CP-induced ^{7}Be production reaction ^{k}Li(CP, x)^{7}Be where ^{k}Li denotes ^{6}Li or ^{7}Li. The ^{7}Be production reaction rate induced with ^{k}Li R_{Be-7} (1/cm^3) is

$$R_{Be-7} = N_{Li-k} \int_0^{E_{max}} \sigma_{Be-7}(E)\phi_{CP}(E)\, dE, \tag{3}$$

where $N_{\mathrm{Li}-k}$ (1/cm^3) is the atomic density of ^{k}Li and $\sigma_{\mathrm{Be}-7}(E)$ (cm^2) the ^{7}Be production cross-section. The effective ^{7}Be production cross-section σ_{eff} (cm^2) is defined as

$$\sigma_{\mathrm{eff}} = R_{\mathrm{Be}-7}/(\phi_n N_{\mathrm{Li}}), \tag{4}$$

where N_{Li} (1/cm^3) is the total atomic density for both ^{6}Li and ^{7}Li. By assembling Eqs. (1)–(4), we will finally obtain the following formula:

$$\sigma_{\mathrm{eff}} = [(N_{\mathrm{A}} N_{\mathrm{Li}-k} \sigma_{\mathrm{CP}}/N_{\mathrm{Li}}] \int_0^{E_{\max}} \left[\sigma_{\mathrm{Be}-7}(E)\{\mathrm{d}E/\mathrm{d}x(E)\}^{-1} \times \int_E^{E_{\max}} P(E_{\mathrm{CP}})\,\mathrm{d}E_{\mathrm{CP}}\right] \mathrm{d}E. \tag{5}$$

Eq. (5) denotes a partial cross-section, i.e., for the target nuclide A, for the CP and for ^{7}Be production from ^{k}Li. The total effective ^{7}Be production cross-section can be obtained by summing up all the partial cross-sections.

3.2. Estimation of effective ^{7}Be production cross-section in the samples

Effective ^{7}Be production cross-sections for the lithium-containing samples were estimated according to Eq. (5). Table 2 summarizes reactions considered in the estimation. The data for σ_{CP} and $P(E_{\mathrm{CP}})$ for ^{1}H and ^{16}O were taken from JENDL-3.2 [5]. The σ_{CP} and $P(E_{\mathrm{CP}})$ data for ^{6}Li and ^{7}Li were very difficult to calculate because CPs were produced by break-up reactions. Hence, the $\sigma_{\mathrm{CP}}P(E_{\mathrm{CP}})$ data were obtained from Shibata [6] who evaluated nuclear data for ^{6}Li and ^{7}Li with detailed consideration of the break-up reactions. Fig. 2 shows the $\sigma_{\mathrm{CP}}P(E_{\mathrm{CP}})$ data, i.e., energy differential CP production cross-section for ^{6}Li and ^{7}Li. The data for $\sigma_{\mathrm{Be}-7}(E)$ shown in Fig. 3 were taken from literature: the ^{6}Li(d,n)^{7}Be reaction was from Refs. [7,8], the ^{6}Li(t,2n)^{7}Be and ^{7}Li(d,2n)^{7}Be reactions were from Ref. [8] and the ^{7}Li(p,n)^{7}Be reaction was from Refs. [9–11]. The data in Ref. [12] were used for stopping power.

Table 2
Reactions considered to estimate the effective ^{7}Be production cross-section

CP production reactions	Cross-section at 14 MeV [mb]
^{6}Li(n,x)p	85
^{6}Li(n,x)d	104
^{6}Li(n,x)t	28
^{7}Li(n,x)p	5
^{7}Li(n,x)d	10
^{7}Li(n,x)t	314
^{1}H(n,n)p	692
^{16}O(n,p)^{16}N	44
^{16}O(n,d)^{15}N	15
^{7}Be production cross-section	
^{6}Li(*d*,*n*)^{7}Be	
^{6}Li(*t*,2*n*)^{7}Be	
^{7}Li(*p*,*n*)^{7}Be	
^{7}Li(*d*,2*n*)^{7}Be	

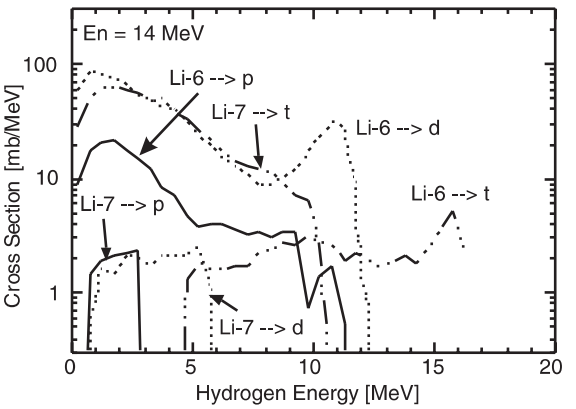

Fig. 2. Energy differential CP production cross-sections for ^{6}Li and ^{7}Li for incident neutron energy of 14 MeV [6].

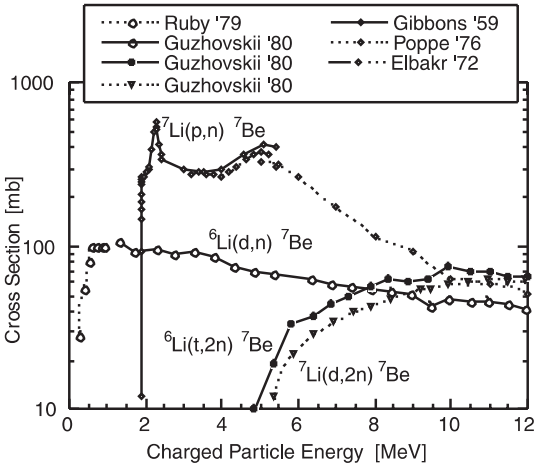

Fig. 3. Beryllium-7 production cross-sections for ^{6}Li and ^{7}Li [7–11].

4. Discussion

4.1. Effective ^{7}Be production cross-section

The experimental cross-sections are shown in Table 1, and Table 3 summarizes the calculated cross-sections along with ratios of calculated to experimental values (C/E). All the C/E values range between 0.62 and 0.99. Although the calculated cross-sections are smaller than the experimental data, the agreement between them is

Table 3
Estimated partial and total effective ^{7}Be production cross-sections and C/E values

Sample	Effective ^{7}Be production cross section [μb] (top: 1st reaction, bottom: 2nd reaction)[a]											C/E
	^{6}Li(n,d) & ^{6}Li(d,n)	^{7}Li(n,d) & ^{6}Li(d,n)	^{16}O(n,d) & ^{6}Li(d,n)	^{6}Li(n,t) & ^{6}Li(t,2n)	^{7}Li(n,t) & ^{6}Li(t,2n)	^{1}H(n,p) & ^{7}Li(p,n)	^{6}Li(n,p) & ^{7}Li(p,n)	^{7}Li(n,p) & ^{7}Li(p,n)	^{16}O(n,p) & ^{7}Li(p,n)	^{6}Li(n,d) & ^{7}Li(d,2n)	Total	
$^{6}Li_2CO_3$	11.7	0.0	0.7	1.5	0.0	–	0.4	0.0	0.4	0.2	14.9	0.93
$^{7}Li_2CO_3$	0.0	0.0	0.0	0.0	0.0	–	0.0	0.1	8.8	0.0	8.9	0.69
$^{nat}Li_2CO_3$	0.1	0.0	0.1	0.0	0.1	–	0.6	0.1	8.1	0.3	9.3	0.62
^{6}LiOH	16.7	0.0	0.7	2.2	0.1	13.1	0.6	0.0	0.4	0.2	33.9	0.97
^{7}LiOH·H_2O	0.0	0.0	0.0	0.0	0.0	469.0	0.0	0.1	9.2	0.0	478.3	0.70
^{nat}LiOH·H_2O	0.0	0.0	0.1	0.0	0.0	434.1	0.5	0.1	8.5	0.2	443.6	0.75
$^{6}Li_2O$	28.8	0.0	0.6	3.8	0.1	–	1.0	0.0	0.3	0.4	34.9	0.71
$^{7}Li_2O·(H_2O)_{0.090}$	0.0	0.0	0.0	0.0	0.0	41.7	0.0	0.2	7.4	0.0	49.4	0.74
$^{nat}Li_2O·(H_2O)_{0.106}$	0.2	0.0	0.0	0.0	0.1	44.9	1.4	0.2	6.9	0.6	54.5	0.99
$^{7}Li_2O$	0.0	0.0	0.0	0.0	0.0	–	0.0	0.2	7.3	0.0	7.5	[b]
^{nat}Li2O	0.2	0.0	0.0	0.0	0.2	–	1.5	0.2	6.7	0.6	9.5	[b]
^{6}Li	60.5	0.1	–	8.0	0.2	–	2.0	0.0	–	0.8	71.7	[b]
^{7}Li	0.0	0.0	–	0.0	0.0	–	0.0	0.5	–	0.0	0.6	[b]
^{nat}Li	0.4	0.1	–	0.0	0.3	–	3.2	0.4	–	1.3	5.9	[b]

[a] The following reactions are excluded from the table because all the partial cross-sections are 0.0: ^{7}Li(n,d) + ^{7}Li(d,2n) and ^{16}O(n,d) + ^{7}Li(d,2n).
[b] No corresponding experimental data.

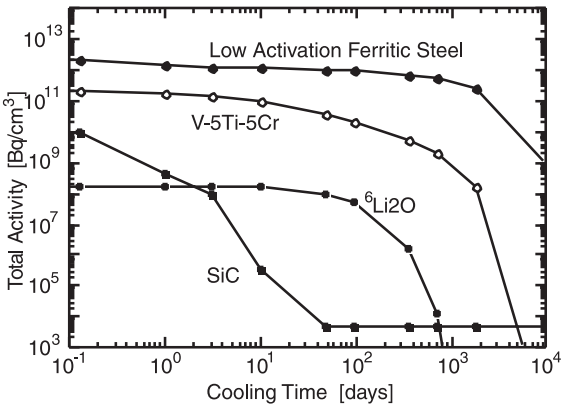

Fig. 4. Total activity of several fusion relevant materials irradiated by 14 MeV neutrons as a function of cooling time.

fairly good. The good agreement indicates that effective cross-sections for SCPR for lithium-containing samples can be estimated adequately by following the presently adopted procedure.

In Table 3, partial cross-sections which are useful for pathway analyses of the ^{7}Be production reaction are also given. For ^{6}Li enriched samples, the ^{6}Li(n,d) + ^{6}Li(d,n) reaction is dominant in producing ^{7}Be. For ^{7}Li enriched samples, following a certain proton production reaction, the ^{7}Li(p,n)^{7}Be reaction is dominant. When a ^{7}Li enriched sample contains hydrogen, such as the $^{7}LiOH \cdot H_2O$ sample, many protons are produced by the elastic scattering reaction of ^{1}H, and this enhances significantly the ^{7}Li(p,n)^{7}Be reaction. When a ^{7}Li enriched sample does not contain hydrogen but does have oxygen, such as $^{7}Li_2CO_3$ and $^{7}Li_2O$ samples, the ^{16}O(n,p) reaction is the most important reaction to produce protons. When a ^{7}Li enriched sample does not contain hydrogen or oxygen, such as the ^{7}Li metal, the ^{7}Be production is suppressed significantly: the total cross-section is only 0.6 μb.

4.2. Impact on fusion reactor design

When a wall load of 14 MeV neutrons of 1 MW/m^2 and saturation of the ^{7}Be activity are assumed, ^{7}Be activity in lithium-6 enriched Li_2O near first walls will reach about 2×10^8 Bq/cm^3. Fig. 4 compares the total activities of the $^{6}Li_2O$ and some low-activation structural materials irradiated in the same condition as a function of cooling time. When low activation ferritic steel or vanadium-alloy (V–5Ti–5Cr) are used, the ^{7}Be activity in a unit volume of the $^{6}Li_2O$ is much smaller than that of the two structural materials. However, when SiC is used as a structural material, the ^{7}Be activity in a unit volume of the $^{6}Li_2O$ exceeds that of SiC in the cooling time period from 3 to 700 days.

^{7}Be produced by SCPR is the only γ-ray emitting nuclide in lithium-containing samples treated in this study. Moreover, the ^{7}Be activity in lithium-containing materials can exceed the total activity in SiC structural material in a certain cooling time interval. Consequently, careful consideration on the ^{7}Be production by SCPR is required to assess radioactive inventories in lithium-containing D-T fusion blanket materials.

Acknowledgements

The authors would like to appreciate Dr K. Shibata of Nuclear Data Center of JAERI for providing the necessary data. The authors also would like to express their sincere thanks to the operation staff of FNS for their collaboration with using FNS.

References

[1] R.A. Forrest, J.-Ch. Sublet, UKAEA FUS, vol. 358, 1997.
[2] S.W. Cierjacks, P. Oblozinsky, S. Kelzenberg, B. Rzehorz, Fus. Technol. 24 (1993) 277.
[3] Y. Ikeda, C. Konno, H. Maekawa, Nucl. Sci. Eng. 116 (1994) 19.
[4] T. Nakamura, H. Maekawa, Y. Ikeda, Y. Oyama, A D-T neutron source for fusion neutronics experiments at the JAERI, in: Proceedings of the International Ion Engineering Congress-ISIAT '83 & IAPT '83, Kyoto, Japan, 12–16 September 1983, pp. 567–570.
[5] T. Nakagawa et al., J. Nucl. Sci. Technol. 32 (1995) 1259.
[6] K. Shibata, private communication, 1999.
[7] L. Ruby, R.V. Ryle, Y. Wong, Nucl. Sci. Eng. 71 (1979) 280.
[8] B.Y. Guzhovskii et al., Izv. Akad. Nauk SSSR, Ser. Fiz. 44 (1980) 1983.
[9] J.H. Gibbons, R.L. Macklin, Phys. Rev. 114 (1959) 201.
[10] S.A. Elbakr et al., Nucl. Instrum. and Meth. 105 (1972) 519.
[11] C.H. Poppe et al., Phys. Rev. C 14 (1976) 438.
[12] H.H. Andersen, J.F. Ziegler, Hydrogen Stopping Powers and Ranges in All Elements, Pergamon, New York, 1977.